

Measurement of air gap thickness underneath an opaque film by pulsed photothermal radiometry

Cite as: Appl. Phys. Lett. **49**, 1761 (1986); <https://doi.org/10.1063/1.97236>

Submitted: 30 July 1986 . Accepted: 18 November 1986 . Published Online: 04 June 1998

A. C. Tam, and H. Sontag



View Online



Export Citation

ARTICLES YOU MAY BE INTERESTED IN

[Pulsed photothermal radiometry for depth profiling of layered media](#)

Applied Physics Letters **51**, 2076 (1987); <https://doi.org/10.1063/1.98985>

[A generalized model of photothermal radiometry](#)

Journal of Applied Physics **53**, 5392 (1982); <https://doi.org/10.1063/1.331468>

[Thermal conduction at a contact interface measured by pulsed photothermal radiometry](#)

Journal of Applied Physics **63**, 4505 (1988); <https://doi.org/10.1063/1.340146>

Hall Effect Measurement Handbook

A comprehensive resource for researchers

Explore theory, methods, sources of errors, and ways to minimize the effects of errors



AIP
Publishing

Measurement of air gap thickness underneath an opaque film by pulsed photothermal radiometry

A. C. Tam and H. Sontag

IBM Almaden Research Center, 650 Harry Road, San Jose, California 95120

(Received 30 July 1986; accepted for publication 18 November 1986)

We describe an experimental method to detect and measure a thin air gap between an opaque film and a substrate. The method is pulsed photothermal radiometry with signal shape analysis at suitable delayed times. This relies on the use of a short light pulse to heat up the surface of the opaque film by $\sim 10^\circ\text{C}$, and detecting the infrared thermal emission from the surface as a function of time for a sufficiently long time. A numerical computation as well as an analytical approximation is developed to explain the dependence of the photothermal radiometry signal shape on the air gap thickness in the range of ten to hundreds of microns. Our work has applications not only for detecting subsurface air gaps and delaminations, but also for measuring the thermal resistance between layers for nondestructive characterization of adhesion bond strengths.

Pulsed photothermal radiometry (PPTR) relies on the use of a short optical pulse to quickly heat up a sample, and the detection of the transient thermal radiation from the sample surface. Similar to pulsed photoacoustic sensing techniques,¹ PPTR has applications in spectroscopy, coating thickness measurement and powder aggregation detection,² thin-film thickness or thermal diffusivity measurements,³ pigment characterization,⁴ and fiber composite strength characterization.⁵ While past work has concentrated on uniform materials or surface layers, recently, investigations of layered structures or composite materials have appeared.⁶⁻⁸ This letter examines the PPTR signal for a layered structure of an opaque film separated from a thick substrate by an air gap of thickness δ . The PPTR signal shape at certain delay times from the excitation pulse is found to be sensitive to the value of δ up to a few hundred micron. We show how the signal shape can be deconvoluted to give δ , thus providing a quantitative nondestructive tool for delamination mapping. Also, since a small air gap behaves in essence like a thermal resistance R , the present technique can also be used to quantify the value of R between a coating and the substrate; if we expect that R is related to adhesion strength (with R decreasing for better adhesion), the measurement of R also provides a new nondestructive detection method for adhesion strengths.

The experimental arrangement is shown in Fig. 1. The sample film is polycarbonate of $20\ \mu\text{m}$ thickness containing 27% carbon black particles. The film is mounted flat and one side is irradiated by an unfocused 8 ns pulse from a nitrogen laser (pulse energy 1 mJ). At the back, the air gap between the film and a given backing material (quartz or germanium with polished surfaces) is controlled to $1\ \mu\text{m}$ accuracy by a piezoelectric translator (Burleigh Inchworm). The center of the uniformly heated region is imaged onto a dc coupled HgCdTe detector (sensitive from 7 to $12\ \mu\text{m}$) using an off-axis parabola mirror and a ZnSe lens, with a Ge plate in the collimated part of the beam to suppress nitrogen laser stray light. The transient PPTR signal is recorded on a transient waveform recorder (Analogic Data 6000) and processed on an IBM PC.

Maximum surface temperatures reached immediately after absorption of the nitrogen laser pulse are $< 20\ \text{K}$ above room temperature T_0 . After 2 ms however, the temperature is almost constant across the film and less than $0.4\ \text{K}$ above T_0 . Under these conditions convection is not expected to affect our measurements, which are taken on a time scale of 100 ms. On this time scale, lateral heat diffusion within the film can be neglected, since the laser spot is large ($2\ \text{cm}^2$ in area) and rather uniform.

To calculate the PPTR signal at later times for our experimental setup, we consider first the following approximate analytical model. Figure 2 gives the model with the temperature profiles at initial ($t = 0$) and later ($t > 0$) times. If the thermal resistance of the film is much smaller than that of the air gap, the temperature drop within the film will be negligible after a short time, and we can therefore use an average film temperature T_f . The semi-infinite backing material has a high thermal diffusivity, such that the surface temperature is not raised significantly above the ambient temperature T_0 . Heat loss of the film is then governed by the heat flow through the air gap, driven by the temperature gradient $T_f - T_0$. Taking into account radiation losses, the heat loss per unit area from the film is

$$-ch\dot{T}_f = [(\lambda/\delta) + 8\sigma\epsilon T_0^3](T_f - T_0), \quad (1)$$

where c is the film heat capacity, h is its thickness, λ the

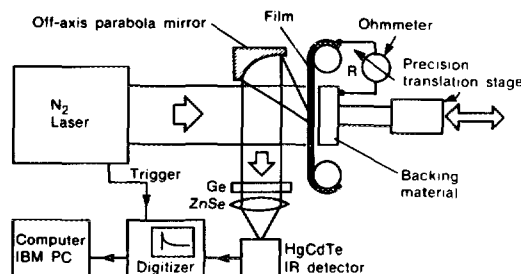


FIG. 1. Experimental arrangement to show PPTR measurement of air gap thickness between a thin opaque film and a thick backing material (substrate). The position of contact between the backing and the film is determined by measuring the electrical resistance between the conducting film and the backing.

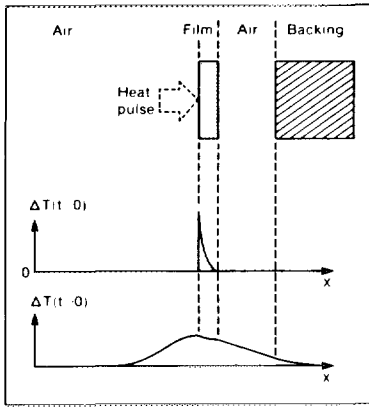


FIG. 2. Temperature distributions in the vicinity of the opaque film at time = 0 (i.e. immediately after the short excitation laser pulse) and at a later time.

conductivity of air, δ the width of the air gap, σ is the Stefan-Boltzmann constant, and ϵ is the film emissivity. Equation (1) can be solved to yield

$$T_f = T_0 + T_e \exp\left(-\frac{(\lambda/\delta) + 8\sigma\epsilon T_0^3}{ch} t\right), \quad (2)$$

where T_e is the initial averaged film temperature rise. From Eq. (2) it is obvious that for a known film thickness h , the gap width δ can be determined quantitatively by analyzing the slope of the radiometry signal on a logarithmic plot. It also turns out that for air as a gap medium, radiation loss is smaller than heat conduction loss for an air gap less than ~ 1 mm. Since most of our investigations have been performed on air gaps less than $200 \mu\text{m}$, radiation losses can be neglected here.

Deviations from the above approximation become apparent under two circumstances: (i) the thermal diffusivity of the backing material is small, causing appreciable surface heating of the backing material and smaller heat flux com-

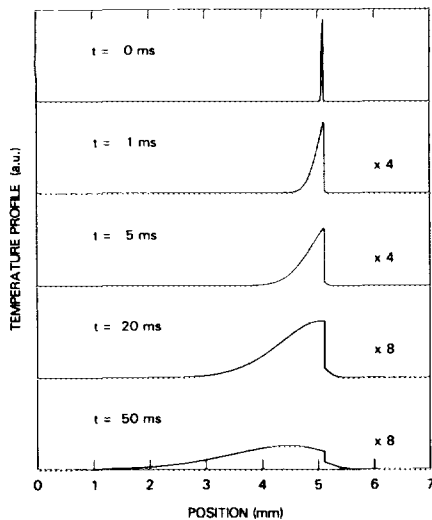


FIG. 3. Computed temperatures in the neighborhood of a $20\text{-}\mu\text{m}$ thin film (at position $x = 5.1$ mm) separated from a germanium substrate by an air gap of $50 \mu\text{m}$ thickness. Neither the thin film nor the air gap can be resolved on the present horizontal scale. The temperature profile for position $x < 5.1$ mm is for the air in front of the thin film, while the profile for $x > 5.1$ mm is for the Ge substrate.

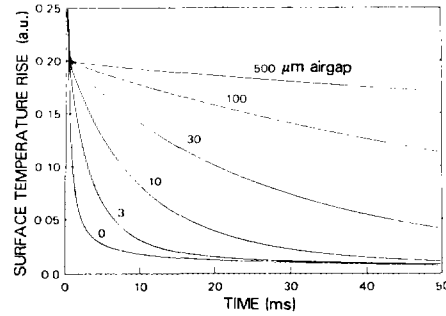


FIG. 4. Computed film surface temperature variations for the case of Fig. 3. The surface temperature, at $t = 0$, is normalized to be unity.

pared to Eq. (1); as a result, the film stays hotter at later times; (ii) for small air gaps, the temperature variations in the film and in the backing cannot be neglected any more. To account for these cases, we have chosen a numerical procedure employing the explicit finite-difference formula technique.⁹ We define $T_{ij} = T(x_i, t_j)$ as the temperature at position $x_i = x_0 + \sum_{v=1}^i \delta_v$ and time $t_j = j\tau$. Here, δ_v is the separation between points x_{i-1} and x_i and is a constant within a homogeneous medium, while τ is the time interval in the calculation process. Within a homogeneous medium, characterized by a thermal diffusivity D , the temperature at position x_i and time t_{j+1} is iteratively calculated as

$$T_{i,j+1} = T_{i,j} + (D\tau/\delta_v^2)(T_{i-1,j} - 2T_{i,j} + T_{i+1,j}). \quad (3)$$

At an interface, the heat flux must be conserved. For the case of a continuous temperature profile, this yields the interface temperature as

$$T_{s,j+1} = \alpha T_{s-1,j} - (\alpha + \beta - 1)T_{s,j} + \beta T_{s+1,j}, \quad (4)$$

where

$$\alpha = 2\tau \frac{\lambda_1/\delta_1}{\lambda_1\delta_1/D_1 + \lambda_2\delta_2/D_2}$$

and

$$\beta = 2\tau \frac{\lambda_2/\delta_2}{\lambda_1\delta_1/D_1 + \lambda_2\delta_2/D_2},$$

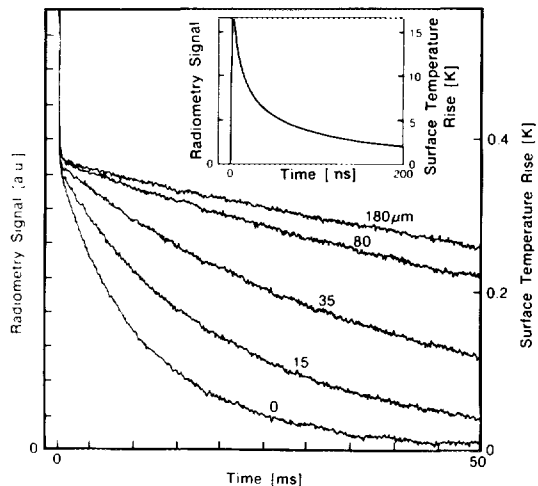


FIG. 5. Observed surface temperature (proportional to the PPTR signal I_R) for a carbon-loaded polycarbonate film at various separations from a germanium substrate.

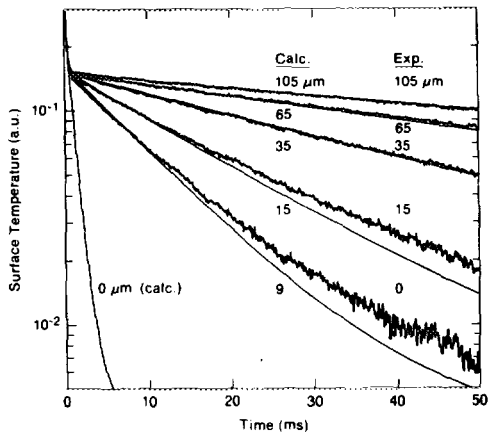


FIG. 6. Comparison between the numerically calculated and experimental PPTR signal I_R for several air gap thickness. The maximum surface temperature is normalized to be unity.

$\lambda_{1,2}$, $D_{1,2}$, and $\delta_{1,2}$ are the thermal conductivity, diffusivity, and x increment in media 1 and 2, respectively. To ensure mathematical stability of this method, the relation $M = D\tau/\delta^2 < 0.5$ should hold for each layer.⁹

Figure 3 gives the numerically computed temperature profiles for a 20- μm film, separated by a 50- μm air gap from a germanium substrate, at different times after the heating pulse. It is interesting to note that at late times the temperature maximum shifts into the air in front of the film due to the cooling effect on its back. Figure 4 gives the corresponding front surface temperatures of the film as a function of air gap width. Experimentally, we observe the effect of the backing clearly from the long-time decay of the transient radiometry signal. As shown in Fig. 5, the early decay is independent of the air gap width, and is also independent of the film thickness, as the optical penetration depth is much smaller. We can easily distinguish different air gap widths up to 500 μm , with $\sim 1 \mu\text{m}$ accuracy.

Quantitative agreement with the numerical model, however, is only good for air gaps larger than $\sim 30 \mu\text{m}$ in width. Figure 6 gives a comparison between calculated and observed PPTR signal which is proportional to the film surface temperature. It should be noted that the theoretical shape is fully determined by the material properties, and only the amplitude was scaled to compare the two sets of data. While the agreement is very good for large air gaps, it becomes increasingly worse for small air gaps below 30 μm . Several effects, which were not accounted for in the numerical model, cause these deviations. (i) When the air gap

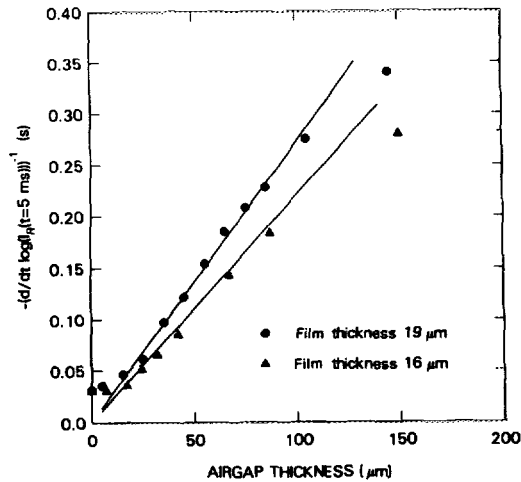


FIG. 7. Dependence of $y = -[(d/dt) \log I_R (t = 5 \text{ ms})]^{-1}$ as a function of air gap thickness δ . Equation (2) indicates that y should be proportional to δ for small radiation losses.

width becomes comparable to the mean free path in air, thermal transport cannot be described by a continuous theory anymore, but is mainly determined by desorption rates from the surfaces involved. (ii) The surface roughness of both film and substrate does not allow a thermal contact at all points; hence, even at 0 μm gap width, there is a thermal interface resistance R . Our data indicate that in our system, with an estimated surface roughness of 1 μm , this thermal resistance corresponds to a 10- μm air layer.

Figure 7 gives a plot of the inverse slope of $\log I_R$ at $t = 5 \text{ ms}$, which according to Eq. (2) should be proportional to both the air gap width and the ribbon thickness. We observe good agreement with the calculated slope [which is a zero parameter fit according to Eq. (2)] over a rather wide range even with the approximate analytical model.

This work is supported in part by the Office of Naval Research.

¹See, for example, A. C. Tam, *Rev. Mod. Phys.* **58**, 381 (1986).

²A. C. Tam and B. Sullivan, *Appl. Phys. Lett.* **43**, 333 (1983).

³W. P. Leung and A. C. Tam, *Opt. Lett.* **9**, 93 (1984).

⁴R. E. Imhof, D. J. S. Birch, F. R. Thornley, J. R. Gilchrist, and T. A. Strivens, *J. Phys. E* **17**, 521 (1984).

⁵P. Cielo, *J. Appl. Phys.* **56**, 230 (1984).

⁶J. Baker-Jarvis and R. Inguva, *J. Appl. Phys.* **57**, 1569 (1985).

⁷J. Baumann and R. Tilgner, *J. Appl. Phys.* **58**, 1982 (1985).

⁸D. L. Balageas, J. C. Krapez, and P. Cielo, *J. Appl. Phys.* **59**, 348 (1986).

⁹J. Crank, *The Mathematics of Diffusion*, 2nd ed. (Clarendon, London, 1975), p. 137.